J|A|C|S
ARTICLES
Published on Web 06/02/2007

A Time-Resolved Electron Paramagnetic Resonance Investigation of the Spin Exchange and Chemical Interactions of Reactive Free Radicals with Isotopically Symmetric (^{14}N−X−^{14}N) and Isotopically Asymmetric (^{14}N−X−^{15}N) Nitroxyl Biradicals

Elena Sartori,[†] Igor V. Khudyakov,[‡] Xuegong Lei,[†] and Nicholas J. Turro*[,†]

Contribution from the Department of Chemistry, Columbia University, New York, New York 10027, and Bomar Specialties, Winsted, Connecticut 06098

Received December 7, 2006; E-mail: njt3@columbia.edu

Abstract: Interactions between reactive free radicals (**r**) with stable mononitroxyl radicals (**N**) and bisnitroxyl radicals (**N**−**X**−**N**) were studied by time-resolved electron paramagnetic resonance (TR-EPR). Reactive spin-polarized free radicals (**r**$^{\#}$), with non-Boltzmann population of spin states were produced by laser flash photolysis of benzil dimethyl monoketal or of (2,4,6-trimethylbenzoyl)diphenyl phosphine oxide (the superscript # symbol indicates electron spin polarization). Both isotopically symmetric nitroxyl biradicals (^{14}**N**−**X**−^{14}**N**) and isotopically asymmetric nitroxyl biradicals, with one nitroxyl bearing ^{15}N and the other nitroxyl bearing ^{14}N (^{14}**N**−**X**−^{15}**N**), were employed as probes of the spin exchange and chemical interactions between **r** and the nitroxyl biradicals. The interaction of **r**$^{\#}$ with the asymmetric *ortho*-nitroxyl biradical (^{14}**N**−**O**−^{15}**N**), which exists in a condition of strong spin exchange, proved to be particularly informative. In this case, spin polarized (^{14}**N**−**O**−^{15}**N**)$^{\#}$ (product of spin exchange with **r**$^{\#}$) and two polarized monoradicals (**r**^{14}**N**−**O**−^{15}**N**)$^{\#}$ and (^{14}**N**−**O**−^{15}**Nr**)$^{\#}$ (products of chemical reaction with **r**$^{\#}$) were observed. The latter three species possess three distinct TR-EPR spectra with different line splittings. The relative cross sections for spin exchange (R_{ex}) and chemical reaction (R_{rxn}) were achieved through computer simulation of the TR-EPR spectra. The cross section for spin exchange, R_{ex}, between **r**$^{\#}$ and (**N**−**X**−**N**) biradical is estimated to be 4−6 times larger than the cross section of chemical reaction, R_{rxn}, between **r**$^{\#}$ and (**N**−**X**−**N**). The *para*-nitroxyl biradical (^{14}**N**−**P**−^{15}**N**) exists in weak spin exchange, and behaves as an equimolar mixture of ^{14}N and ^{15}N mononitroxyls.

Introduction

Bimolecular collisions between two molecules represent one of the most fundamental and common means of inducing chemical reaction and energy exchange between two chemical species. In general, nonreactive collisions between two molecules are "invisible" in the sense that there is no direct chemical manifestation of the event, whereas a reactive collision is "visible" through formation or cleavage of chemical bonds. Electron paramagnetic resonance (EPR) has the potential to detect both the cross sections, R_{rxn}, of chemical reactions (*reactive encounters*) and the cross section, R_{ex}, of spin exchange (*nonreactive encounters*) between two paramagnetic reagents. Nonreactive encounters can manifest themselves in EPR spectra[1−3] owing to different mechanisms involving Heisenberg spin exchange. An encounter of a reactive free radical with another free radical or with a stable biradical leads to a competition between chemical reaction and spin exchange.[4−9] We report a study of the interaction of reactive free radicals **r** with nitroxyl biradicals (**N**−**X**−**N**) by time-resolved continuous wave EPR (TR-EPR) that allows a direct measurement of the ratio of the cross sections R_{rxn} and R_{ex}.

Nitroxyl radicals **N** and (**N**−**X**−**N**) are known to be excellent scavengers of reactive carbon-centered radicals **r**.[10−13a] These

[†] Columbia University.
[‡] Bomar Specialties.

(1) Weil, J. A.; Bolton, J. R.; Wertz, J. E. *Electron Paramagnetic Resonance*; Wiley: New York, 1994.
(2) Gerson, F.; Huber, W. *Electron Spin Resonance Spectroscopy of Organic Radicals*; Wiley-VCH: Weinheim, Germany, 2003.
(3) Molin, Yu. N.; Salikhov, K. M.; Zamaraev, K. I. *Spin Exchange*; Springer-Verlag: Berlin, 1980 (cf., in particular, p. 150).
(4) Bartels, D. M.; Trifunac, A. D.; Lawler, R. G. *Chem. Phys. Lett.* **1988**, *152*, 109.
(5) Savitsky, A. N.; Paul, H.; Shushin, A. I. *J. Phys. Chem. A* **2000**, *104*, 9091.
(6) Jenks, W. S.; Turro, N. J. *J. Am. Chem. Soc.* **1990**, *112*, 9009.
(7) Turro, N. J.; Khudyakov, I. V.; Dwyer, D. W. *J. Phys. Chem.* **1993**, *97*, 10530.
(8) For review articles, see (a) Turro, N. J.; Khudyakov, I. V. *Res. Chem. Intermed.* **1999**, *6*, 505. (b) Nagakura, S.; Hayashi, H.; Azumi, T. *Dynamic Spin Chemistry*; Kodansha-Wiley: Tokyo, 1998. (c) Woodward, J. R. *Prog. React. Kinet.* **2002**, *27*, 165.
(9) Turro, N. J.; Khudyakov, I. V.; van Willigen, H. *J. Am. Chem. Soc.* **1995**, *117*, 12273.
(10) *Controlled Radical Polymerization.* Matyjazewski, K., Ed.; ACS Symposium 685; American Chemical Society: Washington, DC, 1998.
(11) Sobek, J.; Martschke, R.; Fischer, H. *J. Am. Chem. Soc.* **2001**, *123*, 2849.
(12) Denisov, E. T.; Afanas'ev, I. *Oxidation and Antioxidants in Organic Chemistry and Biology*; CRC: Boca Raton, FL, 2005.
(13) (a) Parmon, V. N.; Kokorin, A. I.; Zhidomirov, G. M. *Stable Biradicals*; Nauka Publishers: Moscow, 1980 (in Russian). (b) Parmon, V. N.; Kokorin, A. I.; Zhidomirov, G. M.; Zamaraev, K. I. *Mol. Phys.* **1973**, *26*, 1565. (c) Luckhurst, G. R. *Mol. Phys.* **1966**, *10*, 543. (d) Hudson, A.; Luckhurst, G. R. *Chem. Rev.* **1969**, *69*, 191.

Scheme 1. Photogeneration of Spin-Polarized Radicals **r**# from an Aromatic Ketone (**IRG**, Reaction a) and from Phosphine Oxide (**DPO**, Reaction b)

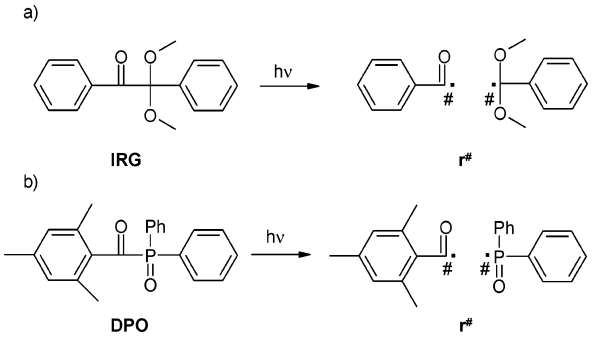

Scheme 2. Competition between Chemical Reaction (Cross Section R_{rxn}) and Spin Exchange (Cross Section R_{ex}) of Reactive Polarized Radical **r**# and a Nitroxyl Radical **N**

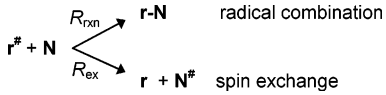

reactions are important from both a fundamental point of view and for practical applications such as inhibition of spontaneous polymerization, controlled free-radical polymerization, and for free-radical chemistry, in general.[10−13a]

In this report we generated spin-polarized reactive free radicals **r**# from suitable precursors according to the reactions shown in Scheme 1 (see Chart 1 for structures of precursors).

The superscript # symbol is used throughout this report to indicate spin polarization, a term applied to situations for which a paramagnetic species possesses a population of spins that is different from the Boltzmann distribution at the temperature of the experiment.

The rates of the competing processes of spin exchange (R_{ex}) and radical combination (R_{rxn}) have been studied in literature by TR-EPR (Scheme 2).[6,7,8a,9] In addition, the relative rates of self-termination of **r**# and of their spin exchange were also studied by TR-EPR and FT TR-EPR.[4,5]

We describe a new method for the estimation of R_{ex}/R_{rxn}, namely, the measurement of relative integrated intensities of TR-EPR spectra corresponding to species which undergo both spin exchange and reaction.[7,8a,9] The ratio R_{ex}/R_{rxn} is a fundamental quantity of considerable theoretical interest[14] since it directly compares cross sections (rates) of two fundamental types of interactions of free radicals with one another: a *chemical* interaction (bond formation) and a *physical* interaction (spin exchange). In the present work we studied TR-EPR of aromatic ketone **IRG** and of phosphine oxide **DPO** in the presence of isotopically labeled nitroxyl biradicals, (**^{14}N−O−^{14}N**), (**^{14}N−P−^{15}N**) and (**^{14}N−O−^{15}N**) (Chart 1).

Experimental Section

1. EPR Experiments. All experiments were performed at ambient temperature. The TR-EPR measurements were obtained with a Bruker ER 100D X-band spectrometer. Samples were excited with light pulses (λ = 308 nm, 10 ns, 10−15 mJ/pulse) from a Physik Lextra 50 XeCl excimer laser. Irradiation took place in a flow flat quartz cell (internal thickness of ∼0.3 mm) in a rectangular cavity (ER 4101 STE) of the

Chart 1. Structures and abbreviations of **N**, **(N−X−N)** and of aromatic ketone (**IRG**) and phosphine oxide (**DPO**), which were used to generate reactive free radicals **r**# (cf. Scheme 1).

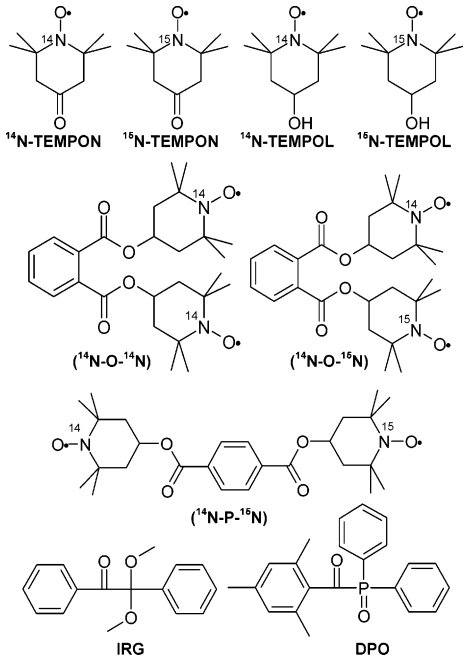

EPR spectrometer. Several transient EPR signals evoked by laser pulses were collected after the microwave bridge preamplifier (20 Hz−6.5 MHz) in the absence of magnetic field modulation. The transient EPR signals were digitized and averaged by a digital oscilloscope triggered on the laser pulse (LeCroy 9450A, 300 MHz) at each of 350 magnetic field values in the sweep of interest. The oscilloscope and the magnetic field advance were computer controlled by a home written LabView program. The experimental technique and basics of TR-EPR are described elsewhere in more detail.[8,15] The signals were acquired at low and high magnetic flux densities and the data matrix was produced by subtracting from each transient a weighted average of the off-resonance signals. The steady-state CW-EPR spectra were recorded with a Bruker EMX EPR spectrometer.

2. Reagents. The following reagents were employed (see Chart 1 for structures): benzil dimethyl monoketal (Irgacure 651, **IRG**) was obtained from Ciba Specialty Chemicals and diphenyl-2,4,6-trimethylbenzoyl phosphine oxide (**DPO**) was obtained from BASF. The following reagents were from Aldrich: benzophenone (BP); phthalic acid; phthalic anhydride; 4-formylbenzoic acid; 2,6-dimethyl-2,5-heptadien-4-one (phorone); 2,2,6,6-tetramethyl-4-oxopiperidinyl-1-oxyl (**^{14}N-TEMPON**) and 2,2,6,6-tetramethyl-4-hydroxy piperidine-N-oxyl (**^{14}N-TEMPOL**); $(^{15}NH_4)_2SO_4$ (98+ atom %), $Na_2HPO_4{\cdot}7H_2O$, NaCl, NaOH, $MgSO_4$, K_2CO_3, oxone (potassium peroxymonosulfate), and all of the solvents. All commercial compounds were used as received.

3. Synthesis of N and (N−X−N). 4-Oxo-2,2,6,6-tetramethyl-1-piperidine-^{15}N (amine) was synthesized by a double Michael addition.[16a] Phorone (9.70 g), $(^{15}NH_4)_2SO_4$ (3.0 g), and benzene (23 mL) were added to a 100 mL glass pressure vessel (Chemglass). The mixture was frozen with acetone/dry ice and then $Na_2HPO_4{\cdot}7H_2O$ (5.5 g) and NaOH (2.3 g) in 7.5 g of distilled water were added. The vessel was immediately sealed and heated to 90 °C in an oil bath with continuous stirring. The reaction was terminated after 10 days and allowed to cool to room

(14) (a) Adrian, F. J. *J. Phys. Chem. A* **2003**, *107*, 9045. (b) Adrian, F. J. *J. Chem. Phys.* **1988**, *88*, 3216. (c) Adrian, F. J. *Res. Chem. Intermed.* **1986**, *7*, 173.

(15) (a) Koptyug, I. V.; Ghatlia, N. D.; Sluggett, G. W.; Turro, N. J.; Ganapathy, S.; Bentrude, W. G. *J. Am. Chem. Soc.* **1995**, *117*, 9486. (b) Turro, N. J.; Khudyakov, I. V. *Chem. Phys. Lett.* **1992**, *193*, 546. (c) Weber, M.; Khudyakov, I. V.; Turro, N. J. *J. Phys. Chem. A* **2002**, *106*, 1938.

(16) (a) Hall, P. L.; Gilchrist, J. H.; Collum, D. B. *J. Am. Chem. Soc.* **1991**, *113*, 9571. (b) Liu, Z. Z. Ph.D. Thesis, Columbia University, New York, 2005.

temperature. The mixture was washed twice with diethyl ether. The ether extract was collected and dried over anhydrous $MgSO_4$. After the filtration, ether was removed under vacuum with the formation of a viscous liquid of amber color. The product was purified by silica gel flash column chromatography, eluting first with a methylene chloride/THF mixture (from 40:1 to 20:1 v/v), and then with a methylene chloride/methanol mixture (from 40:1 to 20:1 v/v). The fraction containing the product was collected and dried under vacuum. 4-Oxo-2,2,6,6-tetramethyl-1-piperidine-^{15}N was obtained in the form of yellow needlelike crystals in a yield of 66%. The structure of 4-oxo-2,2,6,6-tetramethyl-1-piperidine was confirmed by GC, GC/MS (EI), ^{13}C NMR (400 MHz, $CDCl_3$), ^{1}H NMR (300 MHz, $CDCl_3$). **^{15}N-TEMPON** was prepared by the known way of oxidation of 4-oxo-2,2,6,6-tetramethyl-1-piperidine-^{15}N.[16b] The product mixture was purified with silica gel flash column chromatography, eluting with a hexanes/ethyl acetate mixture (from 4:1 to 3:1 v/v). The product was collected as an orange-red solid in 39% yield. GC/MS (EI) *m*/*z* (rel. intensities): 171 (M^+, 100), 172 (39), 152 (24), 141 (35), 115 (48), 83 (61).

4-Hydroxy-2,2,6,6-tetramethyl-1-piperidine-^{15}N (amine) was prepared by reducing 4-oxo-2,2,6,6-tetramethyl-1-piperidine-^{15}N with $NaBH_4$. 4-Oxo-2,2,6,6-tetramethyl-1-piperidine-^{15}N (2.0 g) were dissolved in 35 mL of an ethanol/water mixture (1:1 v/v). The solution was dripped into 10 mL of aqueous solution of $NaBH_4$ (0.25 g) during 6 min while keeping the temperature of the reactive solution at 0 °C (ice/water bath). The reactive vessel was removed from the bath, and the solution was allowed to return to room temperature. NaCl was added to the reaction mixture, and the product was extracted with 50 mL of diethyl ether. The ether fraction was separated with a separation funnel and was dried over anhydrous K_2CO_3. After removal of the solvent at reduced pressure, a white solid of 4-hydroxy-2,2,6,6-tetramethyl-1-piperidine-^{15}N was obtained in 94% yield. The structure of 4-hydroxy-2,2,6,6-tetramethyl-1-piperidine-^{15}N was confirmed by the same methods as those of 4-oxo-2,2,6,6-tetramethyl-1-piperidine-^{15}N described above. **^{15}N-TEMPOL** was synthesized by a similar method as **^{15}N-TEMPON** by oxidation of the corresponding amine. **^{15}N-TEMPOL** was shown to be >98% pure by GC analysis. **^{15}N-TEMPOL** was identified by GC/MS (EI) in a similar way as **^{15}N-TEMPON** described above. The syntheses of **^{15}N-TEMPON** and **^{15}N-TEMPOL** are described in detail elsewhere.[16b]

The nitroxyl biradicals (**N**−**X**−**N**) were prepared as follows. Phthalic anhydride was reacted with **^{14}N-TEMPOL** with the resulting formation of monoester of phthalic acid as described elsewhere.[17] The monoester reacted with **^{15}N-TEMPOL** with the resulting formation of diester (**^{14}N**−**O**−**^{15}N**). The reaction of phthalic anhydride with **^{14}N-TEMPOL** (1:2 on molar basis) yields to diester (**^{14}N**−**O**−**^{14}N**). Esterification of 4-formylbenzoic acid with **^{14}N-TEMPOL** results in 4-hydroxy-2,2,6,6-tetramethylpiperidine-1-oxyl 4-formylbenzoate. The latter was oxidized with oxone to 4-hydroxy-2,2,6,6-tetramethylpiperidine-1-oxyl terephthalic acid monoester, which reacted with **^{15}N-TEMPOL** to form (**^{14}N**−**P**−**^{15}N**). All (**N**−**X**−**N**) were purified by chromatography on a silica gel column with an ether/hexanes mixture (1:3 v/v).

4. Computer Simulation of EPR Spectra. We simulated experimental EPR spectra of mono- and biradicals obtained in this work. For the biradicals, the four uncoupled spin states $|m_S(^{14}\text{N}), m_S(^{15}\text{N})\rangle$ (where m_S has the usual meaning of projection of the electron spin *S*) were taken as basis functions. Zeeman, hyperfine and exchange interaction were calculated on the basis functions for each of the six sets of the m_I (^{14}N), m_I (^{15}N) quantum numbers (where m_I is the projection of the nuclear spin *I*) and the six resulting matrices were diagonalized.[13c,d] Eigenvalues and eigenstates were obtained corresponding to specific values of the two hyperfine interactions $a_{^{14}\text{N}}$, $a_{^{15}\text{N}}$ and of the exchange interaction *J*, chosen to simulate the spectra.

(17) Hassner, A.; Alexanian, V. *Tetrahedron Lett.* **1978**, *46*, 4475.
(18) Komaguchi, K.; Iida, T.; Goh, Y.; Ohshita, J.; Kunai, A.; Shiotani, M. *Chem. Phys. Lett.* **2004**, *387*, 327.

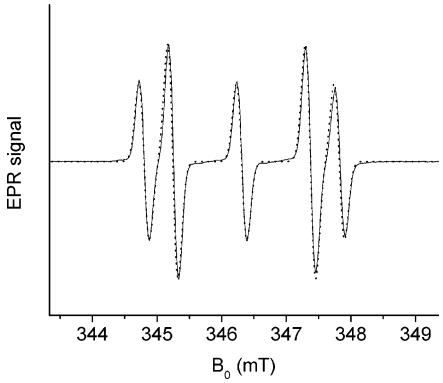

Figure 1. CW-EPR spectrum of (**^{14}N**−**P**−**^{15}N**) (0.5 mM) in hexane (solid line) and its simulation (dotted line).

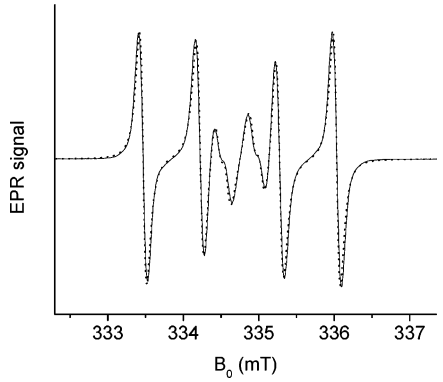

Figure 2. CW-EPR spectrum of (**^{14}N**−**O**−**^{15}N**) (0.5 mM) in hexane (solid line) and its simulation (dotted line).

The field position of the lines depends on the eigenvalues. The ratio of the line intensities derives from the probability of transition, which was obtained from the eigenstates calculated. The spectra were generated by summing of the individual lines which were placed at the proper field, with the proper intensity, width, and shape for each transition.

Spectra of biradicals and monoradicals were summed to simulate the observed TR-EPR spectra and their integrals were calculated. The ratio of integrals of individual spectra contributing to the observed TR-EPR spectra is considered to be equal to the ratio of the concentrations of the corresponding paramagnetic species.

Results

CW-EPR Spectra of Nitroxyl Radicals and Biradicals. The CW-EPR spectra of **^{14}N-TEMPON** [**^{15}N-TEMPON**] were taken in acetonitrile and in hexane. These spectra (not shown) consist, as expected from the literature,[2] of three [two] components with a hyperfine coupling constant $a_N \approx 1.5$ mT [2.1 mT].

Figure 1 displays the CW-EPR spectrum of (**^{14}N**−**P**−**^{15}N**) in hexane. The experimental spectrum of (**^{14}N**−**P**−**^{15}N**) (Figure 1) is the same within the accuracy of our measurements as the EPR spectrum of an equimolar mixture of **^{14}N-TEMPON** and **^{15}N-TEMPON** (or **^{14}N-TEMPOL** and **^{15}N-TEMPOL**). **TEMPO** fragments in (**^{14}N**−**P**−**^{15}N**) are spatially separated; as a result, the exchange interaction, *J*, between unpaired electrons for this biradical is much less than hyperfine coupling constants, a_N.[1,2,13,18] The spectrum (Figure 1) was therefore simulated considering $J = 0$. Throughout this report, we use absolute values of a_N and of *J*.

Figure 2 presents a CW-EPR spectrum of (**^{14}N−O−^{15}N**) in hexane.[19] The spectrum is clearly quite different from that of (**^{14}N−P−^{15}N**) (Figure 1, solid line).

The difference in the spectra of (**^{14}N−P−^{15}N**) and (**^{14}N−O−^{15}N**) is expected to be due to a stronger exchange interaction, J, of the two closely positioned **TEMPO** fragments in the *ortho*-nitroxyl biradical. The latter spectrum was simulated (Figure 2, dotted line) by diagonalization of the Zeeman, hyperfine and exchange interaction (cf. Experimental Section, part 4 above), and summing lines placed at the proper field, with the proper intensity, width, and shape for each transition.

A simple combination of nuclear spins $I = {}^1/_2$ (^{15}N) and $I = 1$ (^{14}N) should lead to a six-component spectrum. However, this result is only a first approximation, valid for $J \gg a_N$. More components arise for smaller J values, and indeed eight components are observed under closer inspection (cf. Figure 2). A value of $J = 24$ mT was obtained from the simulation. The correct intensity of the experimental lines is obtained under the assumption that the intramolecular exchange interaction is modulated by a dynamic process (such as conformational changes of nitroxyl fragments). In fact, to simulate the spectra it is necessary to associate different widths to the EPR transitions that belong to different sets of m_I quantum numbers, which is expected as an effect of the modulation of the exchange interaction J.[13,18] In the classical case of isotopically symmetric nitroxyl biradicals containing only ^{14}N (which possess, therefore, just one hyperfine coupling constant) the effect is null for the transitions occurring between states characterized by two identical m_I, the line width depending on a term $a^2_{^{14}N}(m_I^{(1)} - m_I^{(2)})^2$.[13c,d] The linewidths of the isotopically asymmetric nitroxyl biradicals are expected to depend on the m_I (^{14}N) and m_I (^{15}N) quantum numbers according to a term$(a_{^{14}N}\, m_I\,(^{14}\text{N}) - a_{^{15}N}\, m_I\,(^{15}\text{N}))^2$. Therefore in this case, all of the transitions are affected by the modulation of J, though to a different extent, with those associated with -1, $^1/_2$ and 1, $-{}^1/_2$ being the most affected. They correspond to the central components of the spectrum which are indeed the most broadened.

There are five components expected for the EPR spectra of the (**^{14}N−O−^{14}N**) biradicals in a strong exchange;[1,2,7,13,18] the expected five component spectra were experimentally observed in this work (spectra not shown). The value of J obtained from the simulation for (**^{14}N−O−^{15}N**) was confirmed with the simulation of the spectrum of the isotopically symmetric (**^{14}N−O−^{14}N**), whose lines in fact do not obey the 1:2:3:2:1 ratio expected for $J \gg a_N$. A modulation of J was also necessary in this case to reproduce the experimental intensities.

As for the individual line shape, the Lorentzian line shape leads to the best simulation in the case of (**^{14}N−O−^{14}N**) and (**^{14}N−O−^{15}N**), while Gaussian line shape leads to the best simulation in the case of (**^{14}N−P−^{15}N**). The *para*-nitroxyl biradical (**^{14}N−P−^{15}N**) has a Gaussian line shape (see below) as does the corresponding monoradical (spectrum not shown). This difference in line shapes is consistent with the absence of spin−spin interactions in the *para*-nitroxyl biradical, and the presence of spin−spin interactions in the *ortho*-nitroxyl biradical leads to homogeneous broadening in the latter.

TR-EPR Spectra of IRG and DPO. 2D-TR-EPR spectra produced by photoexcitation of **IRG** and **DPO** were recorded.

(19) We observed minor differences in the CW-EPR spectra of (**^{14}N−P−^{15}N**) and (**^{14}N−O−^{15}N**) in acetonitrile versus hexane. A discussion of these differences is beyond the scope of this work.

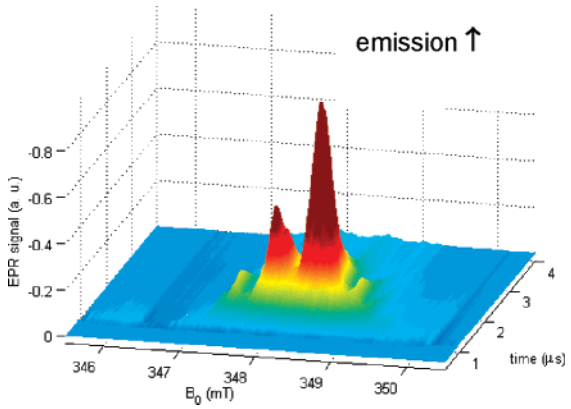

Figure 3. 2D-TR-EPR spectrum produced by photolysis of **IRG** (0.1 M) in acetonitrile.

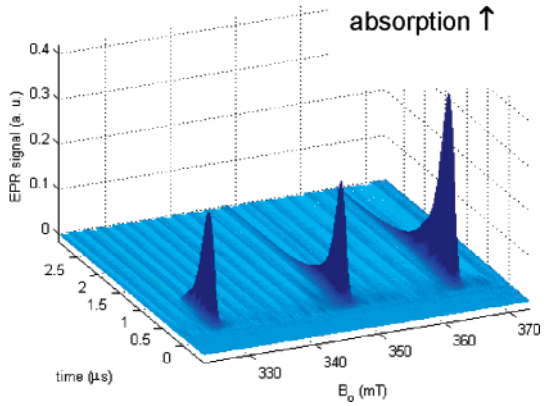

Figure 4. 2D-TR-EPR spectrum produced by photolysis of **DPO** (0.025 M) in acetonitrile.

Photolysis of **IRG** and **DPO** occurs via a triplet state as a Norrish type I process and leads to well-documented TR-EPR spectra of benzoyl and substituted benzyl radicals and of 2,4,6-trimethylbenzoyl and P-centered radicals, respectively (Scheme 1).[7,15b,c,20,21] The radicals **r$^{\#}$** produced by photolysis of **IRG** show strong *emissive* net polarization (Figure 3), whereas the radicals **r$^{\#}$** produced by photolysis of **DPO** show strong *absorptive* net polarization (Figure 4).

The 2D-TR-EPR spectra produced by photolysis of **IRG** and **DPO** (Figures 3 and 4) are consistent with the 1D spectra in the literature. The triplet mechanism (TM) of CIDEP is dominant in the observed polarization for photolysis of **IRG** and **DPO**.[7,8a,15b,c,20,21]

TR-EPR Spectra Produced by Photoexcitation of Benzophenone (BP) in the Presence of ^{14}N-TEMPON and ^{15}N-TEMPON. To extract the cross sections for spin exchange and chemical reaction, R_{ex} and R_{rxn}, the concentrations of radicals must be determined. Thus, an important issue to be addressed is whether the experimental TR-EPR spectra yield the correct relative concentrations of polarized radicals. With this aim, the TR-EPR spectra of **^{14}N-TEMPON$^{\#}$** and **^{15}N-TEMPON$^{\#}$** were obtained by photoexcitation of BP in the presence of an equimolar mixture of **^{14}N-TEMPON** and **^{15}N-TEMPON**. Triplet BP is known to produce emissive polarization of nitroxyl

(20) Jockusch, S.; Landis, M. S.; Freiermuth, B.; Turro, N. J. *Macromol.* **2001**, *34*, 1619.
(21) (a) Makarov, T. N.; Savitsky, A. N.; Möbius, K.; Beckert, D.; Paul, H. *J. Phys. Chem. A* **2005**, *109*, 2254. (b) Forbes, M. D. E.; Yashiro, H. *Macromol.* **2007**, *40*, 1460.

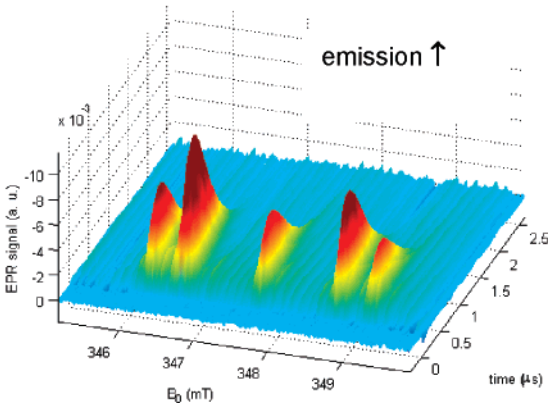

Figure 5. 2D-TR-EPR spectrum produced by photolysis of BP (0.1 M) in the presence of **^{14}N-TEMPON** (0.5 mM) and **^{15}N-TEMPON** (0.5 mM) in acetonitrile.

radicals by the radical triplet pair mechanism (RTPM).[6,8,22] We note that the CW-EPR spectrum of Figure 1 is very similar to the TR-EPR signal of Figure 5, which is an equal molar mixture of **^{14}N-TEMPON** and **^{15}N-TEMPON**. This is the expected result, since isotopic substitution should have a negligible effect on quenching of the triplet state of BP by **TEMPON**.

Isotopic substitution is expected to only influence the EPR pattern of line intensities. However, the low-field components of **^{14}N-TEMPON** and **^{15}N-TEMPON** are found to have somewhat higher intensities than the corresponding high field components (Figure 5) owing to a RTPM multiplet effect.[8,22] We conclude that TR-EPR spectra manifest correct relative concentrations of polarized radicals in the systems reported here.

Photolysis of IRG and DPO in the Presence of (^{14}N−O−^{14}N) and of (^{14}N−O−^{15}N). Figure 6 displays the TR-EPR spectra obtained under photolysis of **IRG** in the presence of (^{14}N−O−^{15}N). The solid line in Figure 6b represents an experimental spectrum extracted from a 2D-TR-EPR spectrum like that in Figure 6a, corrected by subtraction of an experimental spectrum of **IRG** (extracted from a 2D-TR-EPR spectrum of **IRG**). The dotted line in Figure 6b is a simulation based on the weighted sum in eq 1.[7]

$$I_{obs} = a[I((^{14}\mathbf{N}-\mathbf{O}-^{15}\mathbf{N})^{\#})] + 0.5b[I((\mathbf{r}^{14}\mathbf{N}-\mathbf{O}-^{15}\mathbf{N})^{\#})] + 0.5b[I((^{14}\mathbf{N}-\mathbf{O}-^{15}\mathbf{Nr})^{\#})] \quad (1)$$

In eq 1, I_{obs} is the observed intensity of the TR-EPR spectrum (after subtraction of polarized **IRG** contribution, i.e., $\mathbf{r}^{\#}$), $I((^{14}\mathbf{N}-\mathbf{O}-^{15}\mathbf{N})^{\#})$ is the intensity ascribed to $(^{14}\mathbf{N}-\mathbf{O}-^{15}\mathbf{N})^{\#}$, $I((\mathbf{r}^{14}\mathbf{N}-\mathbf{O}-^{15}\mathbf{N})^{\#})$ and $I((^{14}\mathbf{N}-\mathbf{O}-^{15}\mathbf{Nr})^{\#})$ are the intensities ascribed to polarized monoradicals. Integrals of $I((^{14}\mathbf{N}-\mathbf{O}-^{15}\mathbf{N})^{\#})$, $I((\mathbf{r}^{14}\mathbf{N}-\mathbf{O}-^{15}\mathbf{N})^{\#})$ and $I((^{14}\mathbf{N}-\mathbf{O}-^{15}\mathbf{Nr})^{\#})$ are normalized to the same value and the values of a and b were adjusted to fit the experimental spectrum. In the simulated spectrum the component due to $(^{14}\mathbf{N}-\mathbf{O}-^{15}\mathbf{N})^{\#}$ is obtained by using the same parameters (a_{14_N}, a_{15_N} and J) employed to simulate the CW-EPR spectrum of (^{14}N−O−^{15}N) except for the line width, which in general is not expected to be the same as that in TR-EPR spectra. The monoradical components due to $(\mathbf{r}^{14}\mathbf{N}-\mathbf{O}-^{15}\mathbf{N})^{\#}$ and $(^{14}\mathbf{N}-\mathbf{O}-^{15}\mathbf{Nr})^{\#}$ are added to fit the spectra.

(22) (a) Blätter, C.; Jent, F.; Paul, H. *Chem. Phys. Lett.* **1990**, *166*, 375. (b) Kawai, A.; Obi, K. *Res. Chem. Intermed.* **1993**, *19*, 865.

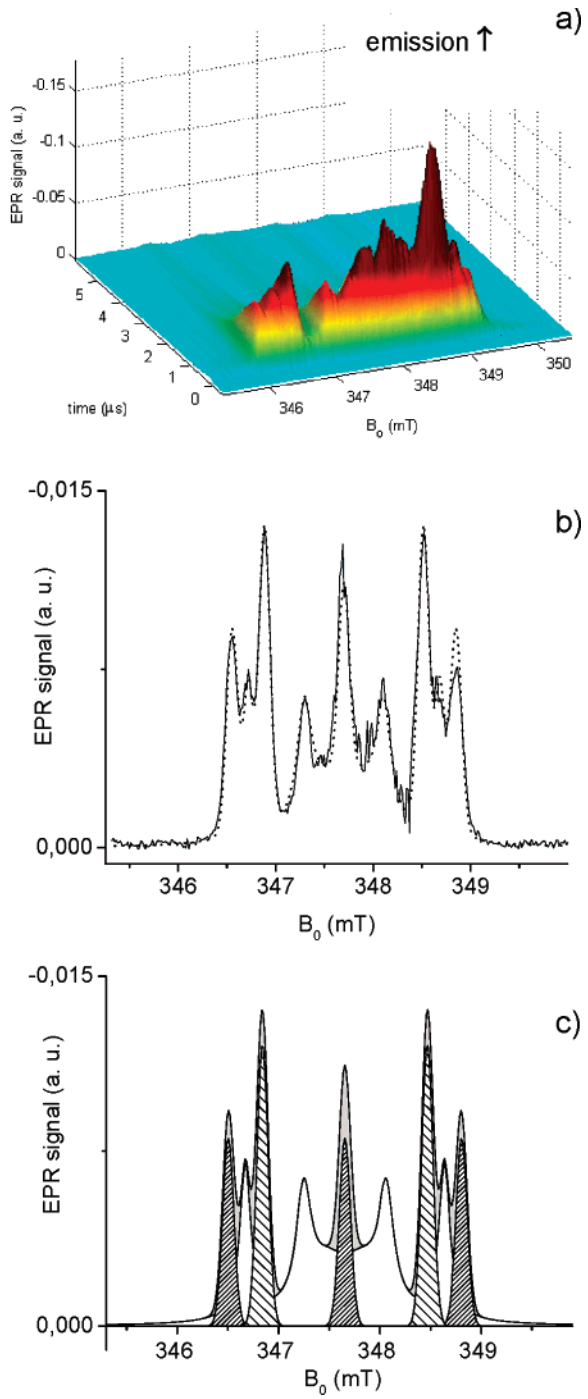

Figure 6. TR-EPR spectra produced by photolysis of **IRG** (0.1 M) in the presence of (^{14}N−O−^{15}N) (1.0 mM) in acetonitrile: (a) 2D spectrum; (b) 1D spectrum at 1 μs after the laser flash (solid line) after subtraction of $\mathbf{r}^{\#}$ (polarized **IRG**) contribution and its simulation (dotted line); (c) relative contributions of each of three polarized species into the simulation spectrum (sparse stripes filling, $(\mathbf{r}^{14}\mathbf{N}-\mathbf{O}-^{15}\mathbf{N})^{\#}$; dense stripes filling, $(^{14}\mathbf{N}-\mathbf{O}-^{15}\mathbf{Nr})^{\#}$, white filling, $(^{14}\mathbf{N}-\mathbf{O}-^{15}\mathbf{N})^{\#}$, gray filling, sum of the three contributions; see the text for discussion). Spectra belonging to different experiments have been chosen for Figure 6a and 6b according to their suitability for 2D and 1D representation.

Table 1 summarizes the a/b values obtained by simulation of the experimental data. The simulation of the experimental spectrum is good but not perfect because of inaccuracies in the subtraction of $\mathbf{r}^{\#}$ contribution into the observed spectrum (Figure 6b). All TR-EPR spectra of spin-adducts $(\mathbf{rN}-\mathbf{O}-\mathbf{N})^{\#}$ are satisfactorily approximated as symmetric spectra. We assume

Table 1. Ratio of Products of Interaction of $\mathbf{r}^{\#}$ with (**N**−**O**−**N**) and Ratio of the Exchange Cross Section to the Reaction Cross Section

biradical	a/b[a]	R_{ex}/R_{rxn}[b]
(^{14}**N**−**O**−^{15}**N**)	1.6−1.1	∼4
(^{14}**N**−**O**−$^{-4}$**N**)	2.4−1.6	∼6

[a] Range of ratios of integral of biradical (**N**−**O**−**N**$^{\#}$) signals to integral of a sum of monoradical (**rN**−**O**−**N**)$^{\#}$ signals (cf. eq 1, 2). Determination error of individual value was 15%. Parameters were obtained by computer simulation of TR-EPR spectra. [b] The estimation of R_{ex}/R_{rxn} is based on a number of assumptions. See the text for discussion.

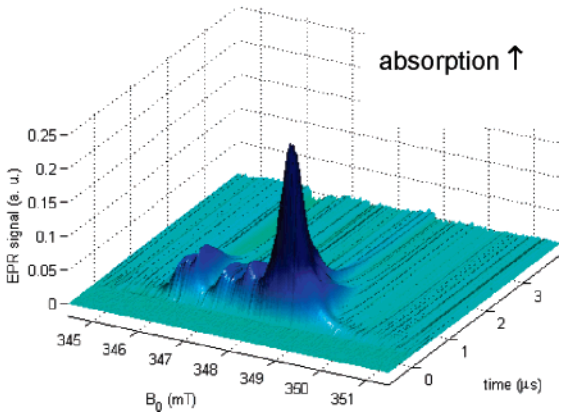

Figure 7. 2D-TR-EPR spectrum produced by photolysis of **DPO** (0.025 M) in the presence of (^{14}**N**−**O**−^{15}**N**) (1.0 mM) in acetonitrile.

that the TR-EPR spectra of $\mathbf{r}^{\#}$ are the result of only action of TM. In the presence of relatively high concentration of spin acceptor, the polarization pattern is preserved in the spin-adduct.[15b,c] The accuracy of such an assumption can be seen by inspection of the goodness of the simulated fit of Figure 6b.

A representative TR-EPR spectrum obtained by photolysis of a solution containing **DPO** and (^{14}**N**−**O**−^{15}**N**) is shown in Figure 7. The TR-EPR spectrum obtained by photolysis of a solution containing **IRG** and (^{14}**N**−**O**−^{14}**N**) is shown in Figure 8.

TR-EPR spectra resulting from the photolysis of **DPO** in the presence of (^{14}**N**−**O**−^{15}**N**) show a residual contribution of $\mathbf{r}^{\#}$ (Figure 7), which makes estimations of relative contributions of paramagnetic species less accurate.

In the case of (^{14}**N**−**O**−^{14}**N**) we used eq 2 instead of eq 1:[7]

$$I_{obs} = a[I((^{14}\mathbf{N}-\mathbf{O}-^{14}\mathbf{N})^{\#})] + b[I((\mathbf{r}^{14}\mathbf{N}-\mathbf{O}-^{14}\mathbf{N})^{\#})] \quad (2)$$

From this point on we will use the designation (**N**−**O**−**N**), to stand for both (^{14}**N**−**O**−^{15}**N**) and (^{14}**N**−**O**−^{14}**N**). The experimental spectra of (**N**−**O**−**N**) were simulated as described above.

In TR-EPR spectra simulation, Lorentzian line shape was always chosen for the biradical (**N**−**O**−**N**)$^{\#}$ contribution into the spectrum, whereas for the spin-adduct (**N**−**O**−**Nr**)$^{\#}$ contributions both a Lorentzian and a Gaussian line shape lead to satisfactory simulation. A certain range of values of a/b (Table 1), rather than a unique value, is obtained depending on whether Gaussian or Lorentzian line shape is ascribed to (**N**−**O**−**Nr**)$^{\#}$ and on some experimental conditions (concentrations and time of observation).

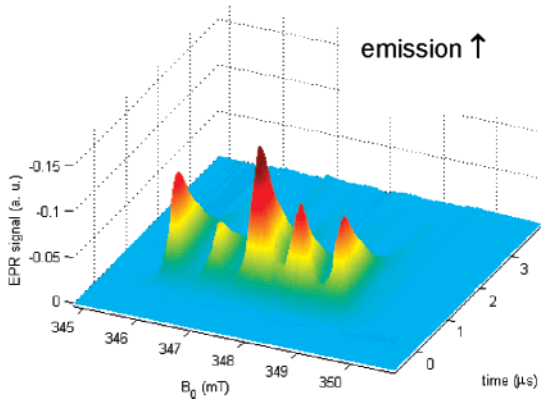

Figure 8. 2D-TR-EPR spectrum produced by photolysis of **IRG** (0.1 M) in the presence of (^{14}**N**−**O**−^{14}**N**) (2.5 mM) in acetonitrile.

Scheme 3. Competition between Chemical Reaction (Cross Section R_{rxn}) and Spin Exchange (Cross Section R_{ex}) of Reactive Polarized Radical $\mathbf{r}^{\#}$ and a Nitroxyl Biradical (**N**−**O**−**N**)

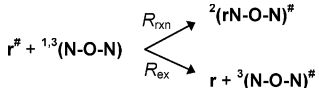

Discussion

Biradicals (^{14}N−X−^{15}N). The biradicals (^{14}**N**−**O**−^{15}**N**) and (^{14}**N**−**P**−^{15}**N**) differ only with respect to the occurrence of different nitrogen isotopes at each nitroxyl center. Six to eight components of the EPR spectrum of (^{14}**N**−**O**−^{15}**N**) are expected according to the value of J for $J > a_N$. As was described above, computer simulation demonstrates excellent agreement with the experimental spectra (Figure 2, dotted line).

Polarization Transfer under Photolysis of Photoinitiators in the Presence of (N−O−N). Scheme 3 is a modified Scheme 2 for a reaction of $\mathbf{r}^{\#}$ with biradical (**N**−**O**−**N**). Knowledge of the relative concentrations of ^{2}(**rN**−**O**−**N**)$^{\#}$ and ^{3}(**N**−**O**−**N**)$^{\#}$ provides a means of determining the ratios of the cross section of spin exchange (R_{ex}) to the cross section of chemical reaction (R_{rxn}), that is, the ratio a/b in eqs 1 and 2.

The (**N**−**O**−**N**)$^{\#}$ is formed by electron spin polarization transfer (ESPT), through the spin exchange.[6,7] The knowledge of experimental a/b ratio allows evaluation of the value of R_{ex}/R_{rxn} under certain assumptions.

In previous experiments[7] with (^{14}**N**−**O**−^{14}**N**) without computer simulation, it was concluded that the magnitude of R_{ex} is close to that of R_{rxn}. The investigation of (^{14}**N**−**O**−^{15}**N**) and computer simulation in experiments with (^{14}**N**−**O**−^{14}**N**) reported here allows us to obtain a more reliable a/b ratio from experimental data. The key feature of our isotopically asymmetric system is that an interaction of a polarized reactive free radical $\mathbf{r}^{\#}$ with (^{14}**N**−**O**−^{15}**N**) results in *three distinct polarized species with different sets of* a_N *for each paramagnetic species and not overlapping spectra* (Scheme 4): ($\mathbf{r}^{14}$**N**−**O**−^{15}**N**)$^{\#}$, (^{14}**N**−**O**−^{15}**Nr**)$^{\#}$ and (^{14}**N**−**O**−^{15}**N**)$^{\#}$. This situation is essentially different from the previously studied case of (^{14}**N**−**O**−^{14}**N**), where the components of the EPR spectrum of (^{14}**N**−**O**−^{14}**N**)$^{\#}$ coincide with components of the adduct (^{14}**N**−**O**−^{14}**Nr**)$^{\#}$ (Scheme 3).[7,13,18]

The value of a/b was found to slightly depend on the assumption of the line shape of (**rN**−**O**−**N**)$^{\#}$. The line shape depends upon the mechanism of the line broadening, and it is

Scheme 4. The Three Distinct Spin Polarized Species Produced by the Interaction of Polarized Free Radical $\mathbf{r}^{\#}$ with (^{14}**N**−**O**−^{15}**N**)

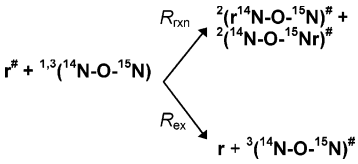

difficult to predict a priori.[1,2,13] This well-known problem is beyond the scope of the present work; however, we can estimate the relative concentrations of paramagnetic species by signal integrals. The values of a/b and R_{ex}/R_{rxn} can be estimated within a certain error (Table 1). We did not perform a detailed investigation of the dependence of a/b values on solvent, temperature, isotope substitution, source of polarized radicals, etc. However, we note that there are no significant changes in a/b with changes from hexane to acetonitrile or the type of (**N**−**O**−**N**) employed; in addition, the measured a/b values depend only slightly on the time of acquisition after the laser flash, and the a/b values weakly depend on the relative concentration of reagents.

Figures 6−8 clearly demonstrate the existence of a certain amount of polarized (**N**−**O**−**N**)$^{\#}$ species. This observation requires that spin exchange (nonreactive ESPT) must occur with a comparable rate to the rate of chemical reaction between the same species (reactive ESPT).[7,8a,23]

According to Schemes 3 and 4, the ratio of concentration of products of two pseudo-first-order reactions should be given by $a/b = R_{ex}/R_{rxn}$. Since R_{ex}/R_{rxn} is expected to be equal to k_{ex}/k_{rxn}, the value of a/b can be treated as the ratio of two rate constants, one for spin exchange and one for chemical reaction. Thus, the measured integrated intensity of (**r**N−**O**−**N**)$^{\#}$ and (**N**−**O**−**N**)$^{\#}$ in TR-EPR experiments are directly proportional to the corresponding pseudo first-order rate constants, k, of their formation. We assume that the relaxation times $T_{1,2}$ of (**r**N−**O**−**N**) are equal to the corresponding $T_{1,2}$ of (**N**−**O**−**N**). CW-EPR measurements demonstrated that consumption of (**N**−**O**−**N**) during the course of the measurement in the flow system was at most a few percent, so that the concentration of ^{1,3}(**N**−**O**−**N**) can be considered as constant during the measurements. In the case of the formation of ^{2}(**r**N−**O**−**N**)$^{\#}$ we need to account for a contribution of a reaction of $\mathbf{r}^{\#}$ with the EPR "invisible" singlet biradicals, ^{1}(**N**−**O**−**N**), which constitute $\sim^1/_4$ of the total concentration of ^{1,3}(**N**−**O**−**N**):[1,7,13]

$$\mathbf{r}^{\#} + {}^1(\mathbf{N}-\mathbf{O}-\mathbf{N}) \rightarrow {}^2(\mathbf{rN}-\mathbf{O}-\mathbf{N})^{\#} \qquad (3)$$

Reaction 3 leads to a concentration of polarized monoradicals that must be considered in our quantitative analysis of R_{ex} and R_{rxn}. Reaction 3 is spin-allowed.

Reaction 4 with EPR "visible" ^{3}(**N**−**O**−**N**), which constitutes $\sim^3/_4$ of the total concentration of (**N**−**O**−**N**),[7,11,13] also leads to polarized monoradicals:

$$\mathbf{r}^{\#} + {}^3(\mathbf{N}-\mathbf{O}-\mathbf{N}) \rightarrow {}^2(\mathbf{rN}-\mathbf{O}-\mathbf{N})^{\#} \qquad (4)$$

The spin-statistical factor for reaction 4 of the doublet $\mathbf{r}^{\#}$ with the triplet ^{3}(**N**−**O**−**N**) is $\sigma_{rxn} = {}^1/_3$.[7,24,25] The rate of addition of $\mathbf{r}^{\#}$ to (**N**−**O**−**N**) is expected to be diffusion-controlled or very close to diffusion-controlled.[7,11,12] The rate constant of a diffusion-controlled reaction occurring on every encounter between highly reactive species, in the absence of spin selection and steric limitations, is described by the von Smoluchowski equation:[3,4,24,26]

$$k_{diff} = 4\pi R_{rxn} D \qquad (5)$$

where D is the mutual diffusion coefficient. In this common approach, the reagents are considered as hard spheres of a certain van der Waals radius, and a reaction occurs under their contact at a distance equal to the cross section of the reaction or the sum of van der Waals radii of reagents R_{rxn}.[26] Thus, the total rate constant of formation of ^{2}(**r**N−**O**−**N**)$^{\#}$ is given by[25]

$$k_{rxn} = 4\pi R_{rxn} D({}^1/_4 + {}^3/_4\,{}^1/_3) \qquad (6)$$

where $^1/_4$ stands for the relative concentration of the singlet ^{1}(**N**−**O**−**N**), $^3/_4$ stands for the relative concentration of the triplet ^{3}(**N**−**O**−**N**) and $^1/_3 = \sigma_{rxn}$.

Equation 7 gives the rate constant of the spin exchange, k_{ex}, in the absence of steric limitations:[3,26]

$$k_{ex} = \sigma_{ex}\,{}^3/_4 4\pi R_{ex} D \qquad (7)$$

We assume in all cases that spin exchange is "strong" or "fast," that is, $J^2\tau^2 \gg 1$, where J is, in this case, the exchange integral between ^{3}(**N**−**O**−**N**) and $\mathbf{r}^{\#}$ and τ is the time of encounter of $\mathbf{r}^{\#}$ and ^{3}(**N**−**O**−**N**).[3,13] The coefficient $^3/_4$ in eq 7 is the fraction of the total concentration of (**N**−**O**−**N**) participating in the spin exchange. The maximum value of σ_{ex} is expected to be $^2/_9$.[3] (Additional comments on the value of σ_{ex} can be found in the Supporting Information.)

The above analysis leads to the expression for the a/b ratio:

$$a/b = [{}^2/_9\,{}^3/_4 4\pi R_{ex} D]/[4\pi R_{rxn} D({}^1/_4 + {}^3/_4\,{}^1/_3)] \qquad (8)$$

or

$$R_{ex}/R_{rxn} = 3a/b \qquad (9)$$

Equation 9 allows the estimation of approximate values of R_{ex}/R_{rxn} (Table 1). If, in fact, reactions 3 and 4 occur with rates lower than diffusion rates, then one needs to use eq 10 instead of eq 6:[26a,27]

$$k_{rxn} = 4\pi R_{rxn} D({}^1/_4 + {}^3/_4\,{}^1/_3) f_{chem} \qquad (10)$$

where $0 < f_{chem} < 1.0$ is the probability of a chemical reaction during the encounter.[26a,27] Then eq 9 should be replaced by

$$R_{ex}/R_{rxn} = 3a f_{chem}/b \qquad (11)$$

(23) RTPM is not responsible for polarization of nitroxyls under photolysis of **DPO** and **IRG** because these two compounds have extremely short-lived triplet states (cf. ref 7 and references therein).

(24) Khudyakov, I. V.; Serebrennikov, Yu. A.; Turro, N. J. *Chem. Rev.* **1993**, *93*, 537.
(25) Buchachenko, A. L.; Ruban, L. V.; Step, E. N.; Turro, N. J. *Chem. Phys. Lett.* **1995**, *233*, 315.
(26) Bimolecular chemical reactions and spin exchange with participation of sterically hindered nitroxyl radicals are often characterized by a certain steric factor f_{eff}, see for example: (a) Burshtein, A. I.; Khudyakov, I. V.; Yakobson, B. I. *Prog. React. Kinet.* **1984**, *13*, 221. See also (b) references 3 and 12. We assume that f_{eff} values are close to each other for reaction and for spin exchange and f_{eff} values cancel each other in eq 9.
(27) Heming, M.; Roduner, E.; Reid, I. D.; Schneider, J. W.; Keller, H.; Odermatt, W.; Patterson, B. D.; Simmler, H.; Pümpin, B.; Savić, I. M. *Chem. Phys.* **1989**, *129*, 335.

Values of R_{ex}/R_{rxn} of approximately 4−6 were determined for the interaction between reactive radicals $\mathbf{r}^{\#}$ and stable nitroxyl biradicals (**N**−**O**−**N**) (eq 9, Table 1). The values of R_{ex} versus R_{rxn} are fundamental parameters for an understanding of reactive and nonreactive contacts between two molecules, an issue of great significance in chemistry. It was concluded in pioneering work[4] on this problem that R_{ex} is 2−3 times larger than R_{rxn} for a reaction between two radicals.[5] The conclusion that R_{ex} will generally be greater than R_{rxn} is understandable: spin exchange can take place when orbitals of reagents overlap weakly, or exchange can occur even through diamagnetic solvent molecules.[3] On the contrary, formation of a covalent bond requires substantial overlap of orbitals of the reacting pair and cannot occur if an intervening molecule separates **r** and (**N**−**O**−**N**). The value of R_{ex}/R_{rxn} may be relatively high. It is possible that reactions are not completely diffusion-controlled, and the use of eq 11 will lead to smaller R_{ex}/R_{rxn} values.

Conclusions

The relative values of R_{ex} versus R_{rxn} were calculated employing TR-EPR and computer simulation to estimate the concentrations of products of spin exchange and chemical reaction between the same reagents.[7,9] It was assumed that the exchange is "strong" and chemical reactions are diffusion-controlled. A unique feature (Scheme 4) of the isotopically asymmetric biradical (**^{14}N**−**O**−**^{15}N**) allows the extraction of values of the ratio R_{ex}/R_{rxn} to be ∼4 from the TR-EPR results. Thus, we conclude that spin exchange between a biradical (**N**−**O**−**N**) and a polarized organic radical $\mathbf{r}^{\#}$ occurs at a relatively large distance. If k_{rxn} is lower than k_{diff}, then an estimation of 4−6 is found as an upper limit of R_{ex}/R_{rxn}.

The study of TR-EPR with computer simulation of spectra of the new biradicals (**^{14}N**−**O**−**^{15}N**) as well as spectra of the known (**^{14}N**−**O**−**^{14}N**) biradicals during photolysis of aromatic ketones has provided a deeper understanding of chemical and physical processes with the participation of biradicals. In addition to the fundamental importance of these measurements toward an understanding of reactive and unreactive collisions, the results and conclusions presented in this report provide an understanding of the mechanisms and chemistry of nitroxyl biradicals. The latter are used as antioxidants and UV-stabilizers of polymers and interact with reactive thermo- or photogenerated free radicals.[12,13a] Finally, we propose that isotopically asymmetric biradicals such as (**^{14}N**−**O**−**^{15}N**) will find new applications as spin probes.

Acknowledgment. The authors thank the National Science Foundation, Grant 04-15516, for generous support of this research.

Supporting Information Available: Additional information on σ_{ex}. This material is available free of charge via the Internet at http://pubs.acs.org.

JA0687670